water

MDPI

Article

Water Geochemistry and Inorganic Quality: Case of the Lower Rusizi Plain Aquifer, North-Western Burundi

Pierre Claver Ngenzebuhoro [1,*], Alain Dassargues [2], Tarik Bahaj [3,*] and Othmane Hammani [4]

[1] Natural and Environmental Sciences Research Center, Department of Earth Sciences, University of Burundi, Bujumbura 1550, Burundi
[2] Hydrogeology & Environmental Geology, Urban and Environmental Engineering Unit, University of Liège, 4000 Liège, Belgium; alain.dassargues@uliege.be
[3] Geosciences, Water and Environment Laboratory, Mohammed V University in Rabat, Rabat 10100, Morocco
[4] Faculty of Sciences, Department of Chemistry, Moulay Ismail University Meknes, Meknes 50050, Morocco; othmane.hammani@hotmail.com
* Correspondence: ngenzeclaver@gmail.com or pierre-claver.ngenzebuhoro@ub.edu.bi (P.C.N.); t.bahaj@um5r.ac.ma (T.B.)

Abstract: The present study area is an alluvial plain consisting of fine clayey sand and coarse sand with mixed lithology. In September 2018, a water sampling campaign was carried out in 28 wells spread all over the plain. The interpretation of the results from the physicochemical analysis allows determination of the hydrogeochemical behaviour and quality of the groundwater sampled in this plain. The spatial distribution of physical and chemical parameters reveals a clear demarcation between the east and the west of the study area. Water samples from wells located in the western part of the plain show a high mineralisation with high electrical conductivity and total dissolved solids. Water samples from the southern and eastern parts show intermediate to low mineralisation. Graphical representations of chemical analysis in the Piper diagrams reveal that the groundwater in the study area can be classified into five families. The evaluation of water quality shows that concentration values of some ions like Na^+, Ca^{2+}, Mg^{2+}, Cl^-, HCO_3^- and SO_4^{2-} are generally high in the western part of the plain along the Rusizi River with very high values particularly observed in the Rusizi delta.

Keywords: physico-chemical parameters; groundwater quality; WHO standard; lower Rusizi plain; Burundi

check for updates

Citation: Ngenzebuhoro, P.C.; Dassargues, A.; Bahaj, T.; Hammani, O. Water Geochemistry and Inorganic Quality: Case of the Lower Rusizi Plain Aquifer, North-Western Burundi. *Water* **2024**, *16*, 1712. https://doi.org/10.3390/w16121712

Academic Editors: Weiying Feng, Fang Yang and Jing Liu

Received: 22 May 2024
Revised: 5 June 2024
Accepted: 13 June 2024
Published: 16 June 2024

1. Introduction

As a crucial source of freshwater on Earth, groundwater plays a vital role in supplying human demands and sustaining the ecological environment [1–3]. The aquifer of the lower Rusizi plain is one of the largest and most important aquifers in Burundi, providing water resources for domestic, agricultural and industrial uses [4]. This plain has known the use of groundwater since the 1950s. Drilling was carried out along transversal tracks for a supply of drinking water to the population who were installed there for the cultivation of cotton [5]. More than seventy wells were drilled in this plain between 1953 and 1960 [5,6]. Some chemical data for only three water samples were found in the bibliography [6], so the hydrogeochemical properties of the groundwater of this area were poorly known until 2018, the year in which sampling was carried out.

Another drilling campaign was started between 2007 and 2015. Thus, some samples of groundwater were collected from 28 new wells and have been analysed in the Laboratory of Hydrogeology, Geophysics and Environment, Applied Sciences Faculty, University of Liège in Belgium (HE-ULiege laboratory). The treatment of the physico-chemical results obtained after laboratory analysis of the 28 groundwater samples leads to determining the concentrations of major and minor elements in the sampled groundwater, as well as determining the reactions with the geological formations in which the water flows. These concentrations were used to determine the inorganic quality of the water sampled.

The main objective of this study is to characterise the physico-chemical properties of the groundwater in the lower Rusizi plain by determining the physical and chemical parameters, their spatial distribution using minimum standards for chemical analysis of groundwater, water facies, hydrogeochemical properties, saturation indices and the inorganic quality of the groundwater compared with the standard drinking water limits established by the World Health Organization (WHO).

2. Materials and Methods

2.1. Location and Geological Setting

The study area lies between the south latitudes of 3°03′00″ to 3°21′00″ and the east longitudes of 29°12′00″ to 29°27′00″. The Lower Rusizi Plain is bordered (Figure 1) to the west by the Rusizi River, which is the natural border between Burundi and the Democratic Republic of Congo (DRC), to the north by the Nyamitanga River, from the north-east to the south-east by the Mirwa foothills and to the south by Lake Tanganyika and the Ntahangwa River.

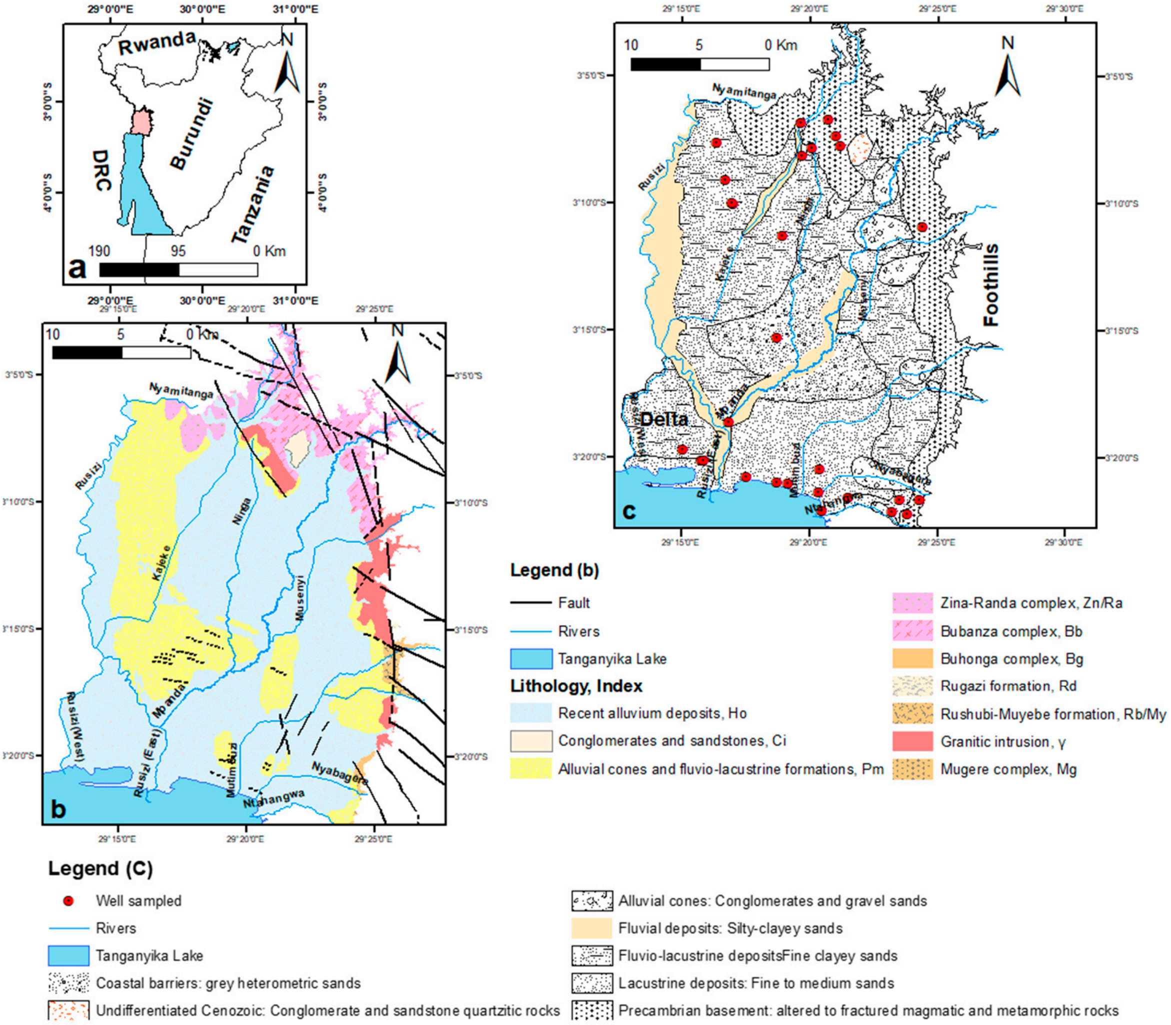

Figure 1. (**a**) Location map of the study area in Burundi; (**b**) geology of the study area: modified from the geological map of Burundi, Bujumbura sheet [4–9]; (**c**) lithostratigraphic description of the aquifer layer of the sampled wells.

The geology of the Lower Rusizi Plain is largely made up of recent Cenozoic formations [7] and another less represented part is made up of Precambrian rocks [8] that border the plain to its eastern limit. The Precambrian outcrops lie on the eastern border [9] while the fluvio-lacustrine alluviums occupy the rest of the area [10,11]. The Cenozoic is constituted by recent alluvial deposits of the Rusizi River, several tributaries of Lake Tanganyika or the Rusizi and piedmont deposits from the foothills (Ho) which cover the eastern part [6]. It is also constituted by Middle Pleistocene (Pm) formations made up of fluvio-lacustrine alluvium [6–12]. The Precambrian outcrops consist of middle Proterozoic magmatic and metamorphic formations [9] consisting of the complexes of Zina/Randa (Zn/Ra), Bubanza (Bb) and Buhonga (Bg), the Rushubi-Muyebe formation (Rb/My) and the granitic intrusions (γ) as shown in Figure 1b. A small Archean outcrop, the Mugere complex (Mg), is represented in the southeast of the plain (Figure 1b).

Therefore, the sedimentology of the lower Rusizi plain is represented by six facies [4–13] as shown in Table 1 and Figure 1c.

Table 1. Sedimentological description of the Lower Rusizi Plain [4].

Facies	General Lithology
Lacustrine deposits	Fine to medium sand and mineralogical composition made of quartz, feldspar and black minerals.
Coastal barriers	Grey heterometric sands (quartz, feldspar, few micas, without black minerals), related to the combined action of lacustrine currents, waves and wind. They are locally superimposed on lacustrine formations.
Fluvial deposits	Silty clay located along the Rusizi and its delta. To the east, they mix with lacustrine sediments, which are partly eroded by the rivers.
Fluvial deposits	Predominantly clayey, which develop to the northeast and east of the plain, in depressions with flat bottoms, limited on the western edge by slopes controlling the direction of the rivers.
Undifferentiated lacustrine and fluvial facies	Fine clayey sand, located between fluvial and lacustrine deposits.
Alluvial cone facies	Blocks and coarse sand to gravel, recognizable on the eastern side of the plain.

2.2. Hydrogeology

Two main drilling periods (1953–1960 and 2007–2015) were observed in the study area. During drilling, the depths of the first water inflow were systematically recorded and then, generally, there is a rise of water in the casing up to 15 m at the completion of the well [4–6]. This phenomenon can be explained by the lenticular layers of the aquifer partially confined by low permeability formations [6–14]. The depth to water measured in the wells, the thicknesses of the aquifer and the layer of clay that confines this aquifer are variables [4]. The thickness of the aquifer is relatively low in fluvial deposits (1 to 6 m) but is increased in littoral barriers and lacustrine deposits (more than 12 m) [4].

The results of the pumping tests were used to determine locally the hydrodynamic parameters, such as hydraulic conductivity values [15]. The lithological heterogeneity of the aquifer indicates that the hydrodynamic parameters calculated from interpretation of pumping tests (steady state without piezometers) are localised around the corresponding wells and cannot be generalised over the whole plain [15].

In general, hydraulic conductivity values decrease from south to north and from west to east, and are generally low near the Precambrian foothills [16]. However, this rule is not generalised in the alluvial cones investigated by the wells near the Kajeke and Mpanda rivers, where hydraulic conductivity values range up to 10^{-3} m/s [16]. The lowest values are found towards the eastern limit of the plain, while the highest values are found towards the south-west. The drillings realised in the Precambrian basement present low hydraulic conductivity values (10^{-6} m/s) [16].

The reference piezometric map [4] reveals a general groundwater flow in the aquifer from the Precambrian basement located to the north-east and east of the plain, towards the south-west (Figure 2). The aquifer–river interactions change from one river to another and from one area to another [4]. In the Kajeke River basin, the orientation of the potentiometric curves reflects a drainage of this river by the aquifer, while in the Mpanda River basin, the concavity of the potentiometric curves reflects a drainage of the aquifer by this river. In other rivers, the potentiometric line orientation confirms that those rivers are drained by the aquifer. The concavity of the potentiometric lines oriented towards the east and the north-east, except in the Mpanda River basin, also reflects a lateral recharge of the aquifer from the altered or fractured Precambrian basement. On the contrary, at its western limit, this aquifer is drained by the Rusizi River and, in the south, Lake Tanganyika constitutes its southern outlet.

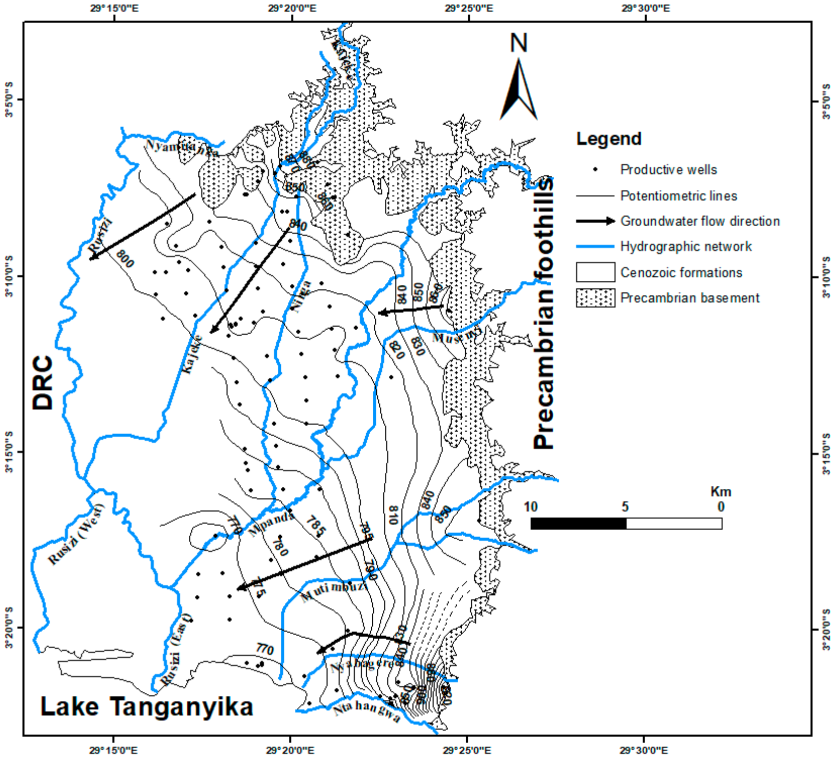

Figure 2. Reference piezometric map of the lower Rusizi plain [4].

2.3. Methodology

Sampling was carried out in September 2018, which is the end of the dry season in Burundi, which normally covers four months (June–September). The sampling methodology adopted was first to identify all the operational wells before starting the water sampling work. Twenty-eight samples were selected from these operational wells. This choice was justified by the easy access to the wells (for example, hand-pumped wells that serve the populations of rural villages are easier to access than private wells, where permission from the owners was a condition for sampling), the possibility of pumping the water for at least thirty minutes to obtain representative water from the aquifer with the aim of having a more or less balanced distribution throughout the study area. The sampling point was taken as representative of the aquifer formation. Field measurements are often carried out for parameters such as pH, electrical conductivity (EC), redox potential (Eh), dissolved oxygen (O_2) and temperature, which are measured by electrodes [17]. In this study, only three parameters (pH, temperature and EC) were measured in situ using a multiparameter (HQ 1110 model manufactured by Hach Lange GmbH, USA) probe in the sampling bucket after rinsing the electrodes with distilled water. In situ EC and pH measures were later compared with those measured in the analysis laboratory. The samples to be analysed in the laboratory were placed in 250 mL plastic bottles. These bottles were then hermetically sealed and placed in sample boxes, which were kept refrigerated until the day of analysis. Table 1 describes the geological formation of the aquifer where the samples were taken, while Figure 1c shows the spatial distribution of samples in different geological formations of the aquifer.

A routine analysis involves measuring the concentration of a standard set of constituents [17]. A standard groundwater chemical analysis as a minimum comprises eleven variables [18] for temperature, electrical conductivity (EC), pH, the four major cations (Na^+, K^+, Mg^{2+}, Ca^{2+}) and four major anions (Cl^-, $HCO_3{}^-$, $SO_4{}^{2-}$, $NO_3{}^-$). The routine analysis typically includes the major constituents with the exception of SiO_2 and carbonic acid, and the minor constituents with the exception of boron and strontium [17]. Major constituents are considered to be those with a volume of concentration higher than 5 mg/L in groundwater, while minor constituents have concentrations between 0.1 and 5 mg/L and the concentrations of all trace elements are lower than 0.1 mg/L [19]. One simple check on the quality of a routine analysis is to compare the sum of concentrations of cations and anions in milli-equivalent per litre [17]. The average electrical balance of groundwater analyses of the lower Rusizi plain is 0.24% with values between 2.6 and 5.9%. These are considered as good quality analyses. Analyses of the four major cations (Ca^{2+}, Mg^{2+}, Na^+, K^+) and anions like Cl^-, $NO_3{}^-$ and $SO_4{}^{2-}$ were realized using a capillary ion analysis (C.I.A) technique. Silica (SiO_2) was analysed by a flame atomic absorption technique, while carbonate ($CO_3{}^{2-}$) and bicarbonate ($HCO_3{}^-$) ions were obtained after determination of pH and the complete alkalimetric title.

The total dissolved solids (TDS) value in mg/L is defined as the mass of the residues divided by the initial volume of water [20]. In this study, TDS was obtained by summing the concentrations of major cations and anions. EC, which is an indirect measure of TDS, reflects the salinity or the mineralisation of groundwater [20]. High values of EC indicate mature waters with long residence times and which have, thus, dissolved the maximum of rock-forming materials [20].

The hydrogeochemistry of major ions is a powerful tool for determining solute sources and for describing the evolution of groundwater after water–rock interaction leading to the dissolution of carbonate minerals, the alteration of silicates and ion exchange processes [21,22]. A high concentration of Na^+ relative to Cl^+ or a decrease in Na^+ relative to Cl^- are clear signs of cation exchange reactions [21]. A Na/Cl ratio approximately equal to and/or less than 1 is generally attributed to halite dissolution [23], whereas a ratio greater than 1 is generally interpreted as reflecting Na released by silicate weathering reactions [23,24]. The chemical data of the groundwater samples were also plotted in Gibbs's diagrams [25].

The equilibrium state of water with respect to a mineral phase can be determined by calculating a saturation index (SI) from analytical data [21,22]. An $SI < 0$ indicates that the groundwater is unsaturated with respect to the mineral considered, while an $SI > 0$ specifies that the groundwater is oversaturated with respect to the mineral phase considered and therefore leading to precipitation of the concerned mineral [21]. If $IS = 0$, the water–rock interaction has reached equilibrium [23,24].

3. Results and Discussion

Table 2 summarizes the major and minor physical and chemical compositions of the groundwater samples while Table 3 shows some chemical reactions between major ions and saturation indices of principal minerals. The sampling point was taken as representative of the aquifer formation.

Table 2. Physico-chemical composition of the groundwater sampled.

Sample ID	EC (μS/cm) [2]	EC (μS/cm) [1]	pH [2]	pH [1]	T	Na^+ (mg/L)	K^+ (mg/L)	Ca^{2+} (mg/L)	Mg^{2+} (mg/L)	Cl^- (mg/L)	HCO_3^- (mg/L)	SO_4^{2-} (mg/L)	CO_3^- (mg/L)	NO_3^- (mg/L)	SiO_2 (mg/L)	TDS (mg/L)	NH_4^+ (mg/L)	Sr^{2+} (mg/L)	F^- (mg/L)
1	4656.8	4200	7.30	6.94	29.9	909.62	48.08	93.50	103.24	281.56	2422.37	453.68	2.67	0.09	52.83	4364.87	50.04	3.22	0.70
2	2487.9	2280	6.81	6.56	29	268.66	30.46	93.07	76.53	91.66	1581.20	6.85	0.56	-	59.65	2208.08	102.69	1.29	0.34
3	7060.8	5960	8.03	7.87	29.4	1543.4	290.90	26.50	92.03	441.35	2515.83	985.04	14.88	515.93	22.99	5918.05	-	0.92	2.54
4	1191.5	1015	6.86	6.62	27.8	28.77	10.32	86.01	55.69	6.05	803.33	7.20	0.32	-	73.13	1070.50	54.35	0.60	0.22
5	549.2	523	7.05	6.95	28.5	45.42	3.07	35.24	17.04	4.41	355.79	105.70	0.22	-	61.64	628.31	14.66	0.25	0.13
6	640.5	644	7.00	6.91	25	66.34	5.27	43.71	22.48	4.35	288.82	105.53	0.16	0.12	36.24	572.74	0.61	0.32	0.35
7	492.0	530	7.30	7.06	25	43.77	1.87	45.97	14.83	3.78	318.92	6.26	0.35	-	58.70	494.09	2.08	0.29	0.27
8	570.7	591	7.19	6.77	28.1	43.06	3.18	65.58	14.23	7.02	354.40	16.56	0.30	-	47.00	551.02	0.50	0.28	0.29
9	289.6	283	6.87	6.65	27.9	36.76	7.61	10.86	8.35	2.43	146.28	26.68	0.06	-	57.71	296.68	-	0.17	0.58
10	693.0	651	7.41	7.51	28.7	84.90	16.19	32.83	26.29	2.77	445.22	15.49	0.63	5.50	50.54	674.23	-	0.28	0.96
11	850.3	801	7.32	7.13	26.8	126.15	7.40	27.39	33.30	9.49	508.76	49.25	0.59	1.22	52.76	814.48	-	0.31	0.97
12	210.3	201	6.57	6.26	27.9	22.24	5.36	11.97	7.42	2.87	119.52	6.39	0.02	0.96	56.49	232.26	-	0.20	0.44
13	738.2	663	7.29	6.87	29.4	56.65	19.47	65.60	24.22	10.83	410.23	26.53	0.44	32.07	64.51	678.04	-	0.53	0.77
14	792.1	791	7.37	6.91	28.2	55.58	6.36	72.16	36.34	8.53	474.54	32.05	0.61	18.78	52.75	738.32	-	0.41	0.68
15	1436.0	1326	7.36	6.92	27.2	185.64	3.99	83.79	58.22	40.21	856.67	66.65	1.08	20.07	58.64	1353.81	-	0.45	1.00
16	723.8	796	7.51	7.12	30.9	78.18	7.61	51.47	26.35	9.08	438.81	30.08	0.78	4.70	37.39	678.97	-	0.34	0.62
17	1879.4	1740	7.31	7.05	31	220.94	8.20	112.19	85.93	39.06	542.87	579.85	0.61	0.57	38.71	1627.73	-	0.62	0.69
18	1585.9	1574	8.17	8.05	28.4	338.25	7.32	27.91	26.82	6.84	818.37	194.80	6.68	23.92	58.35	1478.65	-	0.59	1.59
19	1579.5	1353	7.82	7.4	29.3	326.15	4.54	34.37	31.26	17.40	859.79	164.29	3.13	17.60	69.56	1507.35	-	0.35	0.99
20	1185.0	1065	7.52	7.18	29	108.15	1.27	80.30	66.77	8.97	627.17	173.47	1.15	1.52	72.16	1138.26	-	0.63	0.71
21	714.0	660	7.51	7.19	29.3	83.38	2.28	59.32	18.26	6.36	412.07	54.55	0.74	-	79.22	715.43	1.03	0.31	0.40
22	606.4	577	7.54	7.24	28.4	31.73	2.63	72.17	20.83	16.85	369.42	8.47	0.71	-	60.67	582.76	1.34	0.37	0.34
23	477.7	506	7.21	7.04	28.4	34.16	2.15	51.71	14.91	2.55	303.22	11.15	0.27	-	57.20	477.05	0.48	0.29	0.47
24	763.4	709	7.67	7.42	29.1	50.85	11.45	72.70	26.86	40.57	383.48	13.49	0.99	28.53	82.41	681.82	-	0.48	0.92
25	623.0	520	7.10	6.4	27.6	56.36	11.18	42.26	19.36	45.88	260.71	11.05	0.18	36.98	79.65	526.44	-	0.38	0.62
26	560.1	510	6.94	6.68	27.1	35.24	5.92	45.43	19.09	55.22	156.01	20.64	0.07	56.04	64.08	401.61	-	0.36	0.50
27	564.0	709	6.49	6.6	27.7	34.96	14.35	33.96	14.11	72.70	200.03	3.18	0.03	6.98	62.11	435.39	3.04	0.38	0.36
28	450.1	414	7.04	6.77	29.1	28.92	3.55	44.21	18.18	2.83	280.25	9.19	0.17	2.65	70.32	457.45	-	0.33	0.45

Note: [1] Field measurements; [2] Laboratory analysis.

Table 3. Chemical reactions and saturation index.

Sample ID	TDS (mg/L)	Ca (meq/L)	Na (meq/L)	Cl (meq/L)	Na+K/Na+K+Ca	Cl/Cl+HCO$_3$	SI Calcite	SI Aragonite	SI Dolomite	SI Gypsum
1	4469	4.66	39.55	7.93	0.90	0.17	0.91	0.76	2.16	−0.96
2	2359	4.64	11.68	2.58	0.73	0.09	0.33	0.18	0.88	−2.67
3	6473	1.32	67.11	12.43	0.98	0.23	1.06	0.92	2.98	−1.23
4	1163	4.29	1.25	0.17	0.26	0.01	0.14	0	0.41	
5	575	1.76	1.97	0.12	0.54	0.02	−0.32	−0.47	−0.65	
6	597	2.18	2.88	0.12	0.58	0.03	−0.4	−0.54	−0.77	−1.65
7	533	2.29	1.90	0.11	0.46	0.02	0	−0.15	−0.18	−2.81
8	581	3.27	1.87	0.20	0.37	0.03	0.08	−0.07	−0.2	−2.26
9	333	0.54	1.60	0.07	0.77	0.03	−1.35	−1.49	−2.5	−2.75
10	712	1.64	3.69	0.08	0.71	0.01	0.09	−0.06	0.39	−2.6
11	849	1.37	5.48	0.27	0.81	0.03	−0.04	−0.19	0.32	−2.2
12	268	0.60	0.97	0.08	0.65	0.04	−1.67	−1.82	−3.23	−3.3
13	751	3.27	2.46	0.30	0.48	0.04	0.23	0.08	0.34	−2.08
14	791	3.60	2.42	0.24	0.42	0.03	0.4	0.26	0.83	−1.97
15	1412	4.18	8.07	1.13	0.66	0.07	0.66	0.51	1.48	−1.66
16	708	2.57	3.40	0.26	0.58	0.03	0.38	0.24	0.8	−2.13
17	1654	5.60	9.61	1.10	0.64	0.11	0.49	0.34	1.19	−0.66
18	1547	1.39	14.71	0.19	0.91	0.01	0.98	0.83	2.27	−1.67
19	1571	1.71	14.18	0.49	0.89	0.03	0.74	0.6	1.78	−1.65
20	1186	4.00	4.70	0.25	0.54	0.02	0.69	0.54	1.63	−1.25
21	765	2.96	3.63	0.18	0.55	0.03	0.43	0.28	0.68	−1.8
22	622	3.60	1.38	0.47	0.29	0.07	0.51	0.36	0.82	−2.51
23	513	2.58	1.49	0.07	0.37	0.01	−0.03	−0.17	−0.26	−2.51
24	762	3.63	2.21	1.14	0.41	0.15	0.64	0.5	1.2	−2.33
25	612	2.11	2.45	1.29	0.56	0.23	−0.3	−0.44	−0.6	−2.61
26	497	2.27	1.53	1.56	0.43	0.38	−0.65	−0.79	−1.33	−2.3
27	484	1.69	1.52	2.05	0.53	0.38	−1.1	−1.25	−2.25	−3.23
28	503	2.20	1.26	0.08	0.38	0.02	−0.3	−0.44	−0.64	−2.65

3.1. Physico-Chemical Characteristics of Groundwater

3.1.1. Physical Characteristics

Temperature (Table 2) values range from 25 to 31 °C. In most of the wells sampled (except for samples 6 and 7), the temperature values are higher than the maximum value of the WHO standard (25 °C). The pH values in situ are slightly lower than the pH values measured in the laboratory with the exception of the water in sample 10 (Table 2). The pH values in situ range from 6.26 to 8.05 while pH values measured in the laboratory range from 6.49 to 8.17. Most of the samples analysed present an alkaline characteristic (pH > 7). In the study area, EC varies between 210.3 and 7060.8 µS/cm (EC laboratory) and between 201 and 5960 µS/cm (EC in situ). TDS varies from a minimum of 176.75 mg/L to a maximum of 5918.05 mg/L. Note that for almost of all samples, the EC measured in the field is slightly lower than that measured in the laboratory. According to the EC values, the water sampled in the western part of the study area can be classified as mature water and can reflect the contribution of evaporative concentration, the dissolution of evaporitic salts and anthropogenic pollution.

The high mineralisation observed in the wells drilled in the western part of the plain near the Rusizi River and in the Delta (Figure 3) would be influenced by the infiltration of water from the Rusizi River which is a river with high salinity, as the Rusizi is an outlet of Lake Kivu from the north between DRC and Rwanda, which is a saline lake. For the drillings located in the north-west along the Kajeke River, the high mineralisation observed in the groundwater samples could be a result of the contribution of seepage water from this river with its excess of dolomites [6]. The physico-chemical parameters in the water samples that were collected over the whole extent of the plain show an evolution in water mineralisation from east to west and more particularly in the Rusizi Delta. The different methods used in this work lead us to distinguish three zones: the Rusizi Delta (more mineralised), the western part (intermediate mineralisation) and the less mineralised part from the north-east to the south-east (Figure 3).

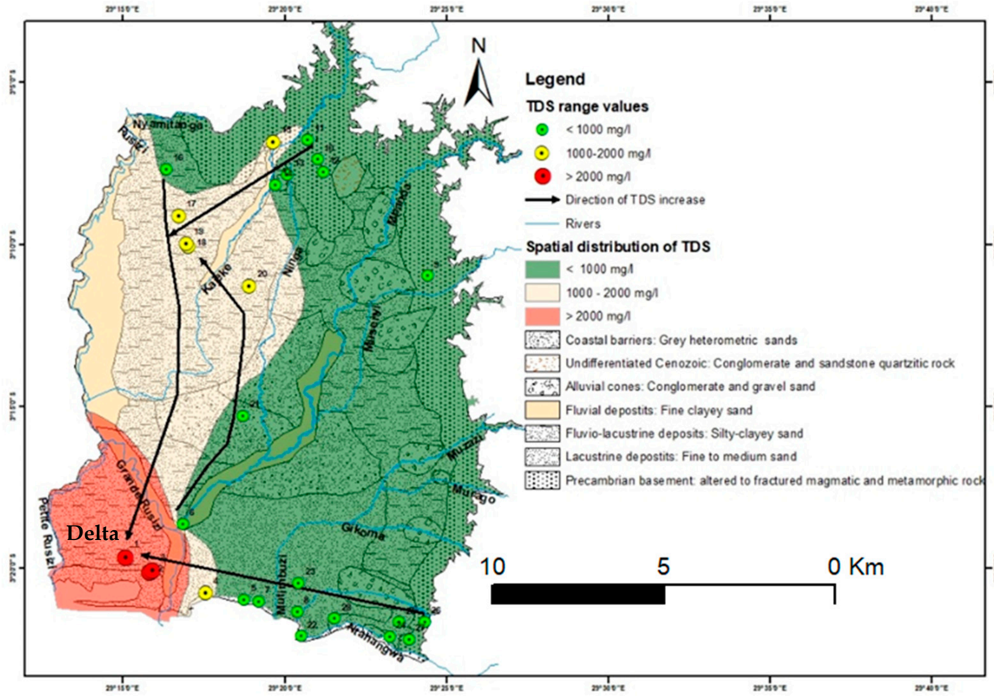

Figure 3. Spatial distribution of TDS with a clear increase from the east towards the west of the lower Rusizi plain.

3.1.2. Major Elements

As the TDS in this study area was obtained by summing the concentrations of major cations and anions, the spatial distribution of major cations and anions shows (Figure 3) an increasing trend from the north-east (basement) towards the south-west (Delta). In the Delta and the western part of the Kajeke River, except for well n°16 (Figure 3), Na^+ is the most dominant cation. The concentration of Na^+ in the groundwater samples varies from a minimum of 22.24 to a maximum of 1543.4 mg/L. The highest concentration of Na^+ occurs in the water samples collected in the Delta (1543.4 mg/L), whereas the lowest concentration is found in the water samples collected in the Precambrian basement (22.24 mg/L). Concentrations of Ca^{2+} and Mg^{2+} are relatively high compared to Na^+ in the south near Lake Tanganyika and the Ntahangwa River. Concentrations of K^+ are absolutely lower, except in the water sample from well n°3 (290.90 mg/L), compared to the concentrations of other major cations.

Except in the groundwater sample from well n°17, HCO_3^- is the most dominant anion. The increase in the spatial distribution of this anion trends from east to the south-west in the Delta, where the highest concentration measured is 2515.83 mg/L in the water samples from well n°3. The concentration of Cl^- varies from a minimum of 2.43 (well n°9) to a maximum of 441.35 mg/L (well n°3). Of the twenty-eight groundwater samples studied, only two samples (n°1 and 3) show Cl^- concentrations exceeding the taste-based limit of 250 mg/L [26]. The spatial distribution of this element shows that there is a general increasing trend from east to south-west (Delta). The spatial distribution of SO_4^{2-} shows an increasing trend from east to west with particularly high concentrations in wells n°1, 2 and 17.

NO_3^-/CO_3^- and SiO_2 are, overall, characterised by low concentrations, except in sample n°3 (515.93 mg/L) for NO_3^-. On the contrary, the concentration of SiO_2 decreases from the east to the west of the plain with the minimum observed in the water sampled from well n°3 (22.99 mg/L).

The overall lowest concentration values of K^+ and Mg^{2+} in the different groundwater samples compared to Na^+ values explain the smaller contribution of K- and Mg-bearing aluminosilicates to the hydrogeochemical evolution of groundwater. In the groundwater samples from the wells in the south of the plain, the highest concentrations of Ca^{2+} denote that the higher contribution of Ca-bearing minerals is significant compared to the other sources of cations. The clear demarcation in concentration values of HCO_3^- between the north-east and south-west parts of the study area confirms that the concentration of HCO_3^- progressively increases along the flow path (Figure 2) as the results of the dissociation of H_2CO_3 in groundwater [19]. The spatial distribution of SiO_2 displays a random variation which does not correspond to the increasing trend from the Precambrian basement towards the Rusizi Delta. Water samples with high mineralisation such as those sampled from wells located in the west part of the plain (TDS > 1000 mg/L) present low concentrations of SiO_2. The relatively high concentrations of silica in the water sampled in wells drilled in the Precambrian basement and alluvial cones confirm the metamorphic origin of this element.

3.1.3. Minor Constituents

Ammonium (NH_4^+) is the most toxic form of nitrogen. Its presence in water is related either to urban and industrial wastes, or the reduction of nitrogenous forms (nitrates and nitrites) under reduced conditions [27]. In the laboratory, NH_4^+ was analysed for only 11 water samples. All these analysed samples were collected in the south of the plain, in the Delta, near Lake Tanganyika and along the Ntahangwa River (Figure 3). High NH_4^+ concentrations were found in the water samples from the wells located in the south-west of the plain, with a maximum of 102.6 mg/L in well n°2. Wells n°1 and 2 are located very close to a former breeding site while wells 4 and 5 are located in the south of the breeding areas. It can be seen that wells with a TDS greater than 1000 mg/L present high NH_4^+ concentrations, such as wells n°1, 2 and 4. The remaining samples analysed were collected in the urban parts of Bujumbura (towards the east) and show low NH_4^+ concentration values. Combining the location of the samples showing high values of NH_4^+ and the farming activities that were carried out near or upstream of the sampling sites, these high NH_4^+ concentrations would be caused by organic origins.

Fluoride (F^-) concentration values in the groundwater samples of the lower Rusizi plain range from a minimum of 0.13 to a maximum of 2.54 mg/L. A high F^- concentration is found in well n°3 located in the Rusizi Delta.

Strontium (Sr^+) is an alkaline earth metal. Sr^+ ion concentrations are high in the south-western part of the plain, particularly in the Rusizi Delta, with values ranging from 0.6 to 3.22 mg/L. Most of the wells present concentration values less than 0.5 mg/L of Sr^+. There is evidence for high Sr^+ concentrations in the Rusizi Delta by correlating the facies illustrated by the Piper diagram related to the presence of evaporate formations with high concentrations of Sr^+ (Figure 4).

3.2. Water Facies

Figure 4 shows the projection of different water samples in the Piper diagram. This diagram allows distinguishing five water families of which $CaMgHCO_3$ and $CaHCO_3$ are the most abundant ones, with respective abundances of 54% and 21%, while $NaKHCO_3$, $NaCaClSO_4$ and $NaKClSO_4$ represent 10, 7%; 10, 7% and 3, 6%, respectively. A visual analysis of the anion and cation triangles of the Piper diagram shows that most of the water samples plot in the bicarbonate type (lower left) and in the no-dominant type (middle), respectively, thereby confirming that HCO_3^- is the most abundant anion, while for cations, we observe the exception for only five samples, of which three plot in the Na+K corner and two in the Mg corner.

The water families illustrated by the Piper diagram are spatially distributed in the study area based on their TDS (Figure 5). Therefore, all samples collected in the western part and in the Delta were plotted in $CaMgClSO_4$, $NaKHCO_3$ and $NaKClSO_4$ with a TDS exceeding 1000 mg/L. In addition to the high mineralisation, these water samples are also characterised by high concentrations of Na^+ (220.94–1534.4 mg/L), Mg^{2+} (26.35–103.24 mg/L), HCO_3^- (542.87–2515.83 mg/L), Cl^- (6.84–441.35 mg/L) and SO_4^{2-} (164.29–985.04 mg/L). Samples collected from wells drilled near Lake Tanganyika in the lacustrine formations were plotted in $CaHCO_3$ with a TDS between 500 and 1000 mg/L. The majority of the samples with low mineralisation that were collected from the north-east to the south-east and in the littoral barriers were plotted in $CaMgHCO_3$.

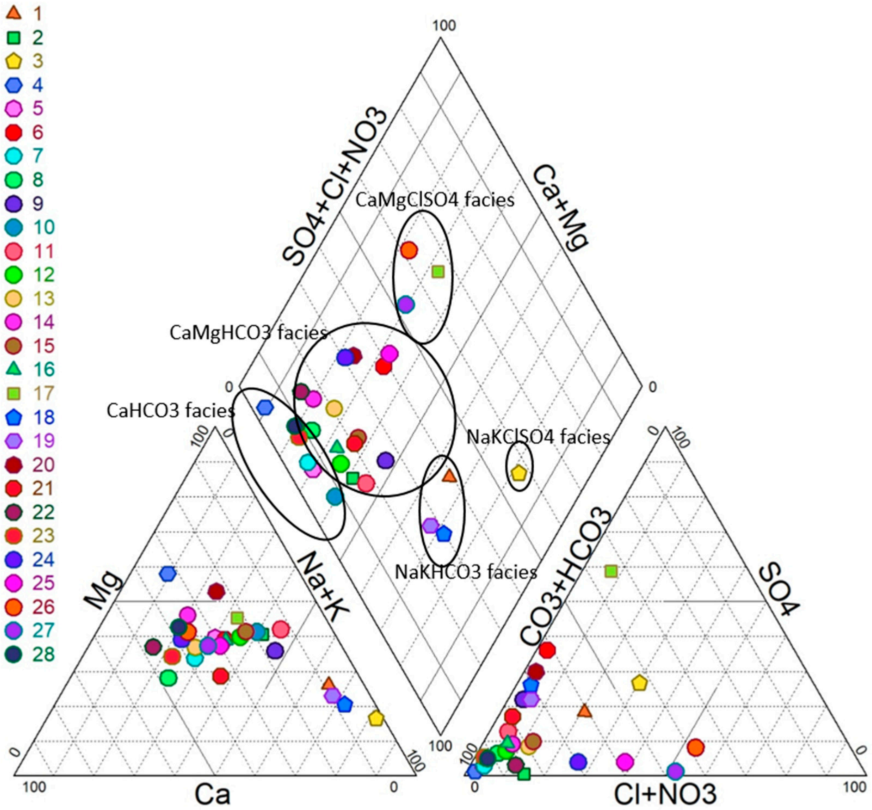

Figure 4. Piper diagram for classifying groundwater of the lower Rusizi plain and defining different chemical types.

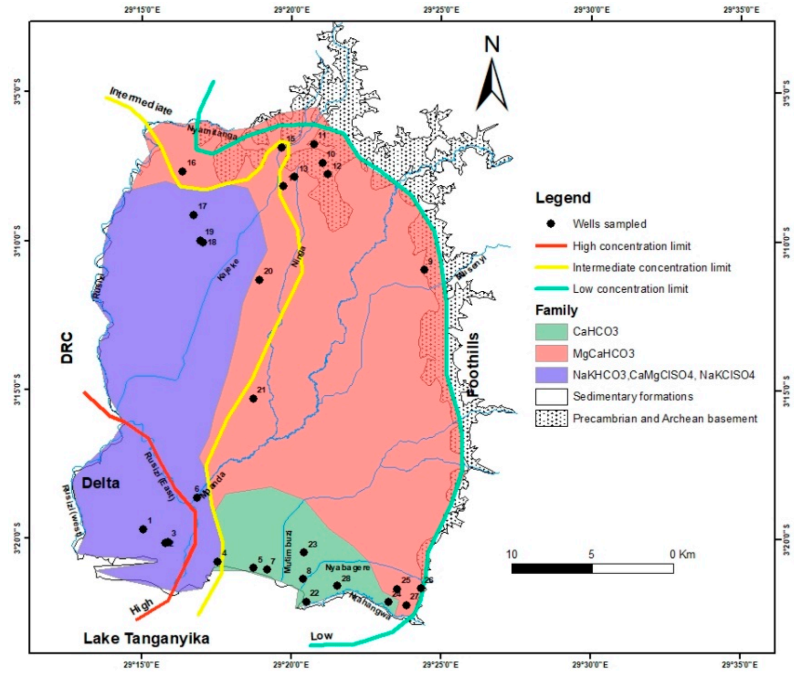

Figure 5. Map showing spatial distribution of water families, major cations and anions, and TDS limit with an increase towards the south-west of the study area.

The Piper diagram allows confirming that most of the groundwater samples have a predominance of $MgCaHCO_3$ facies, that explains that this water flows in fluvio-lacustrine (clayey sand) media. A total of 21% ($CaHCO_3$) flows in a lacustrine environment, while 10, 7% ($NaKHCO_3$) flows in a sand environment. $CaMgClSO_4$ and $NaKClSO_4$ water types explain that the water flows through an alluvial environment with high evaporites.

3.3. Hydrochemical Evaluation

In this study, the results of chemical analysis are used to identify the geochemical processes and mechanisms in groundwater aquifer systems. The results show that most of the samples present a Na/Cl ratio around or below 1 (Figure 6a). A Na/Cl ratio approximately equal to and/or below one is usually attributed to halite dissolution [23], whereas a ratio greater than one is typically interpreted as reflecting Na released from silicate weathering reactions [23–27]. Considering the results shown in Figure 6a, it can be deduced that rain or infiltration/irrigation water is the most likely source of Na and Cl in the study area. Figure 6b shows ion exchange reactions, where Na is plotted against Ca and shows that most of the samples are far below the theoretical line (1:1), indicating the participation of those cations in the ion exchange reaction [21].

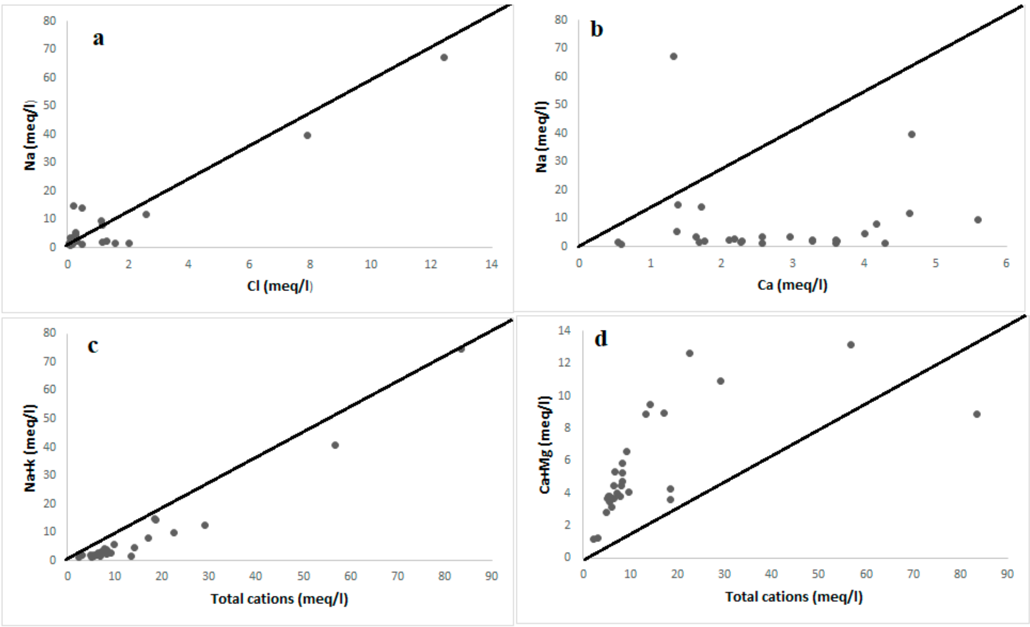

Figure 6. Graphs indicating different parameter chemical processes in groundwater of the study area.

Groundwater sample concentrations are plotted for Ca + Mg and Na + K vs. total cations (Figure 6c,d). Figure 6c shows that all samples are plotted below the theoretical line (1:1), indicating that the supply of cations via ion exchange, silicate weathering and/or soil salts is more significant [21]. On the contrary, Figure 6d shows that most of the samples are plotted far above the theoretical line (1:1), indicating the supply of cations via soil salt dissolution.

By Gibbs diagram, the results show that most of the groundwater samples plot in rock–water interaction and mixing rock–water interaction/evaporation (Figure 7) which indicates that the chemical weathering of rock-forming minerals and evaporation are influencing the groundwater chemical process.

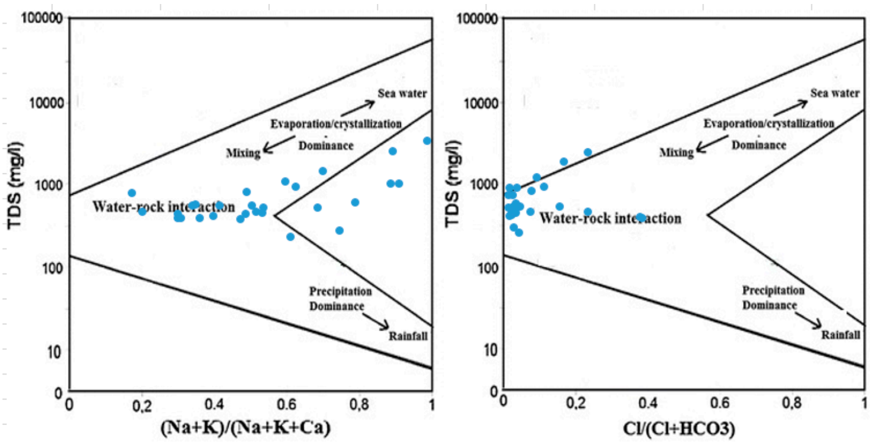

Figure 7. Mechanisms controlling groundwater chemistry in a Gibbs diagram.

3.4. Saturation Index

Table 3 shows the SI of calcite, dolomite, aragonite and gypsum. In this study, the SI of major minerals such as calcite, dolomite, aragonite and gypsum were evaluated (Figure 8). The analysis of the groundwater–aquifer interaction by SI also shows the heterogeneity of the aquifer in the Lower Rusizi Plain. The SI calcite, dolomite and aragonite values are less than 0 for most of the samples collected in lacustrine formations and the Precambrian basement, which means that those minerals could be easily dissolved along the flow path of groundwater. For the samples collected generally in the western part, the SI of calcite, dolomite and aragonite is greater than 0, indicating that the groundwater in this part of the plain is supersaturated with respect to calcite, dolomite and aragonite and is able to form precipitations of these minerals. For gypsum, the SI of gypsum is below zero for all samples, indicating that this mineral could be easily dissolved along the flow path of groundwater.

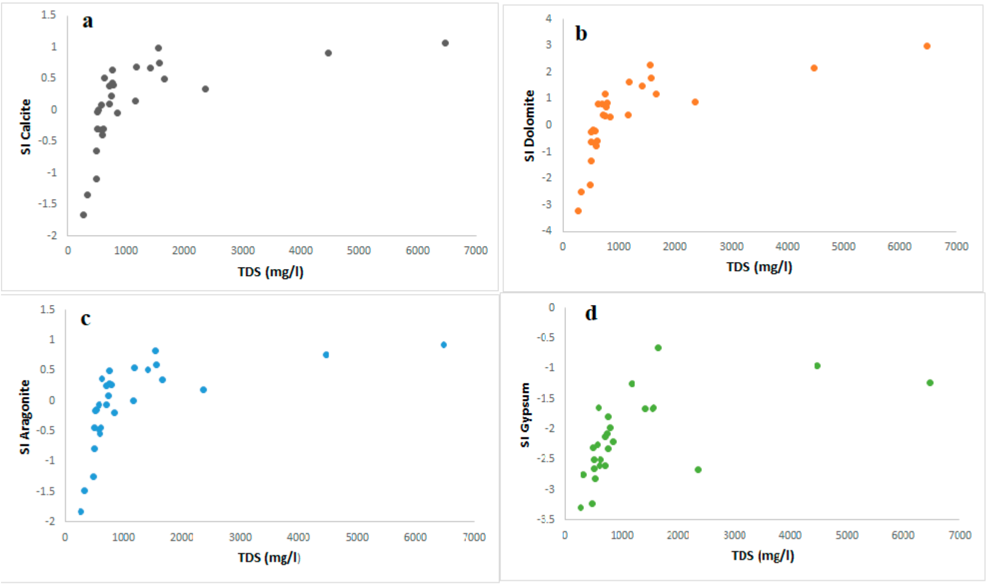

Figure 8. Plots of SI versus TDS.

3.5. Groundwater Quality

Due to the non-existence of national standards for water quality, reference will be specifically made to WHO standards [26]. Referring to Table 2, only one sample shows a pH slightly lower than the standard limits of the WHO (6.5). Of the twenty-eight samples, twenty-one of them show an alkaline character (pH > 7) and the rest have a slightly acidic pH. Among the twenty-eight water samples, twenty-seven of them show pH values within the WHO standards (6.5–8.5) for drinking water.

One basic measure of water quality is the TDS (Table 4) [28]. Groundwater chemistry has been used in this study to assess water quality for drinking, agricultural and industrial purposes.

Table 4. Classification of water based on TDS [28].

Class	TDS (mg/L)	Class	TDS (mg/L)
Fresh	0–1000	Saline	10,000–100,000
Brackish	1000–10,000	Brine	>100,000

There is no exact health-based guideline for TDS, but the WHO fixes an upper limit of 1000 mg/L for drinking water; this value has been set based on taste considerations [21]. Of the twenty-eight samples, nine of them (32%) show TDS values exceeding the taste-based limit and have TDS values between 1070 and 5918.05 mg/L. All these water samples were collected in the western part of the lower Rusizi plain with high values found in the Rusizi Delta samples. The remaining samples are characterised by TDS values lower than 1000 mg/L. According to the classification of groundwater based on TDS, 32% samples are classified in the brackish water category and the remaining samples (68%) are classified as fresh water. From this classification based on TDS, it can be deduced that the north-eastern, central and southern part, respectively in the Precambrian formations, alluvial cones, lacustrine deposits and littoral barriers, contain samples classified as fresh water, while the water sampled in the fluvial formations of the Rusizi and the fluvio-lacustrine formations located in the western part of the study area is classified as brackish water.

Of the twenty-eight water samples studied, six samples present Na^+ levels exceeding the taste-based limit of 200 mg/L. These six samples were collected from wells located in the western part of the study area with a maximum concentration value observed in the Rusizi Delta. The remaining samples show Na^+ levels within the WHO standard limits with low concentration values in the water sampled in the Precambrian basement. For Ca^{2+}, only six samples show concentrations higher than the normal of 75 mg/L with the maximum observed in the west (well 17) and in the Rusizi Delta in wells n°1 and 2. Mg^{2+} concentration values exceed the standard of 50 mg/L in seven samples collected in the western part of the plain, with high values observed in samples collected in the Rusizi Delta. Concentrations values of K^+ are within the recommended limit of 200 mg/L except for the water sample from well n°3 in the Rusizi Delta.

For the Cl^- anion, only two samples (wells n°1 and 3) present Cl^- levels exceeding the taste-based limit of 250 mg/L. Apart from the two samples collected in the Rusizi Delta, which have concentration values significantly exceeding the WHO drinking water limit, the remaining samples analysed present low chloride concentrations, ranging up to concentration values of 5 mg/L. The lowest concentration values were found in the eastern part of the plain in the water sampled in the wells drilled in the Precambrian basement. Concentration values of $SO_4{}^{2-}$ show an increasing trend from east to the south-west in the Delta with particularly high concentration values observed in wells where high concentrations of Cl^- (wells n° 1 and 3) and NO3- (well n°3) are equally found. Of the twenty-eight water samples studied, only three samples (wells n°1, 3 and 17) show concentrations exceeding the WHO taste-based guideline of 250 mg/L. The localised high concentrations of $SO_4{}^{2-}$, which are associated with high concentrations of Cl^- and $NO_3{}^-$, are indicative of anthropogenic pollution [22]. $HCO_3{}^-$ is the most dominant anion with fifteen samples (53.3%) which present concentration values exceeding the taste-based guideline of 400 mg/L. The spatial distribution of $HCO_3{}^-$ concentration shows a clear contrast between the eastern part of the plain where low concentrations are analysed and the western part, particularly in the Rusizi Delta, where very high concentration values

(1581.20–2515.83 mg/L) of this anion occur. NO_3^- and SiO_2 are, overall, characterised by relatively low concentrations except in the water sample n°3 for NO_3^-.

For NH_4^+, the high concentrations are found in the wells located in the south–west with values approximately 100 times higher than the standard of drinking water which is 0.5 mg/L. For the F- ion, only the water sample from borehole n°3 also shows a value exceeding the WHO recommended limit of 1.5 mg/L.

Based on the chemical reactions between the major elements and the Gibbs diagram, it can be seen that different components result from the dissolution of salt soils and that the different minerals are dissolved in the groundwater along the path of the groundwater flow (SI less than 0) and precipitates are generated towards the western outlet of the groundwater. It can also be seen that water quality in the study area is controlled by water–rock interaction, infiltration and evaporation.

4. Conclusions

This hydrogeochemical study of groundwater in the alluvial environment of the lower Rusizi plain was carried out based on the analytical results of twenty-eight water samples. The spatial distribution of physical and chemical parameters reveals a clear demarcation between the east and the west of the study area. Water samples from wells located in the western part of the plain show a high to intermediate mineralisation with high EC and TDS values. Water samples from the southern part near Lake Tanganyika and from the eastern part of the plain show in general a low mineralisation.

Graphical representations of chemical analysis in a Piper diagram reveals that the groundwater in the study area can be classified into five families. The predominance type of $MgCaHCO_3$ reveals that a majority of water samples were collected in wells drilled in fluvio-lacustrine formations (clayey sand).

This study made it possible to establish a spatial distribution of the physico-chemical elements analysed over the entire plain and to identify the types of groundwater that can be found in the wells located in the study area. It also made it possible to assess the quality of groundwater that the population of this area consumes every day. It can be seen that the groundwater of the Rusizi Delta and most of the wells located to the north-west of the plain are highly mineralised in major cations and anions. According to the presence of the different components in the sampled water and their spatial distribution, we can conclude that the western part of the lower Rusizi plain presents groundwater that does not satisfy the standards of drinking water set by the WHO, especially the Rusizi Delta. Samples collected in the Precambrian basement, in the central part and in the south of the plain, show that their concentrations in different ions are lower than the WHO standard limits for drinking water.

For drinking water supply and for various other uses such as animal farming, agriculture and industry, the groundwater of the western part of the plain and particularly the Rusizi Delta is not recommended because of the different concentrations of dissolved ions, which are far higher than the standard limits of the WHO. The remaining part of the plain can be used for groundwater supply, although other analyses not presented in this paper are necessary.

Author Contributions: Conceptualization, A.D. and T.B.; Methodology, O.H.; Writing—original draft, P.C.N.; Writing—review & editing, T.B.; Funding acquisition, A.D. All authors have read and agreed to the published version of the manuscript.

Funding: This research received no external funding.

Data Availability Statement: Data are contained within the article.

Acknowledgments: The authors warmly thank the Laboratory of Hydrogeology and Environmental Geology of the ArGEnCO Department of the University of Liège as well as the Academy of Research and Higher Education of Belgium (ARES). Many thanks also go to Alain Dassargues of the ArGEnCO department of the University of Liège who greatly facilitated these analyses and built a bridge between the first author of this manuscript and the members of his research unit and laboratory. Our thanks also go to Philippe Orban of the ArGenCO department of the University of Liège and to Joël Otten, head of the chemical analysis laboratory of this department.

Conflicts of Interest: The authors declare no conflict of interest.

References

1. Alley, W.M.; Healy, R.W.; Labaugh, J.W.; Reilly, T.E. Flow and storage in groundwater systems. *Sciences* **2002**, *296*, 1985–1990. [CrossRef] [PubMed]
2. Boulton, A.J. Recent progress in the conservation of groundwaters and their dependent ecosystems. *Aquat. Conserv. Mar. Freshw. Ecosyst.* **2009**, *19*, 731–735. [CrossRef]
3. Pan, G.; Li, X.; Zhang, J.; Liu, Y.; Liang, H. Groundwater-flow-system characterization with hydrogeochemistry: A case in the lakes discharge area of the Ordos Plateau, China. *Hydrogeol. J.* **2019**, *27*, 669–683. [CrossRef]
4. Ngenzebuhoro, P.C.; Dassargues, A.; Bahaj, T.; Orban, P.; Kacimi, I.; Nahimana, L. Groundwater Flow Modeling: A Case Study of the Lower Rusizi Alluvial Plain Aquifer, North-Western Burundi. *Water* **2021**, *13*, 3376. [CrossRef]
5. Hakiza, G. Potentialités aquifères de la Plaine de la Rusizi (au Nord du lac Kivu). Ph.D. Thesis, Université de Liège, Liège, Belgium, 2002.
6. Waleffe, A. *Esquisse hydrogéologique de la plaine de la basse Rusizi (Burundi)*; Department of Geology and Mineralogy: Tervuren, Belgium, 1985; annual Report 1983–1984; pp. 177–187.
7. Ilunga, L. Le Quaternaire de la Plaine de la Ruzizi. Etude Morphologique et Lithostratigraphique. Ph.D. Thesis, Vrije Universiteit, Bruxelles, Belgium, 1984.
8. Ntungicimpaye, A. Contribution à l'étude du magmatisme basique dans le kibarien de la partie occidentale du Burundi. Ph.D. Thesis, Ghent University, Ghent, Belgium, 1984.
9. Theunissen, K. On the Rusizian basement rise in the Kibara belt of Northeastern Lake Tanganyika. In *Collision Belt Geometry or Restraining Bend Emplaced in the Late Kibaran Strike-Slip Environment*; IGCP No 255 Bulletin/Newsletter 2; TU Braunschweig and RMCA: Tervuren, Belgium, 1989; pp. 85–92.
10. Ilunga, L. Morphologie, volcanisme et sédimentation dans le rift du Sud-Kivu. *Bulletin de La Société Géographique de Liège* **1991**, *27*, 209–228.
11. Ilunga, L. Environnements sédimentaires et minéralogie des formations superficielles de la Plaine de la Ruzizi (Nord du Lac Tanganyika). *Geo-Eco-Trop* **2007**, *31*, 71–104.
12. Frankart, R.P.; Herbillon, A.J. *Aspects de la pédogénèse des sols halomorphes de la basse Rusizi (Burundi): Présence et génèse de l'Analcime*; Musée Royal de l'Afrique Centrale: Tervuren, Belgium, 1971.
13. Chorowicz, J.; Thouin, C. Failles synsédimentaires et structure de la plaine de la Rusizi (Nord-Tanganyika). *Comptes Rendus L'académie Sci. Série 2 Mécanique Phys. Chim. Sci. L'univers Sci. Terre* **1985**, *301*, 835–840.
14. Snel, M.J. Contribution à l'étude hydrogéologique du Congo belge. Direction Générale Du Service Géologique. *Congo Belg.* **1957**, *2*, 31.
15. Ngenzebuhoro, P.C.; Mohammed, S.; Bahaj, T.; Faouzi, M.; Kacimi, I. *Géométrie et caractérisation hydrodynamique d'un système aquifère plio-quaternaire; Cas de la plaine de la basse Rusizi (Burundi) [Geometry and Hydrodynamical Characterization of a Plio-Quaternary Aquifer System; Case of the Lower Rusizi Plain (Burundi)]*; Bulletin de l'Institut Scientifique; Section Sciences de La Terre: Rabat, Morocco, 2019; pp. 37–53.
16. Ngenzebuhoro, P.-C. Hydrogéologie, Hydrochimie et Modélisation Numérique de l'Aquifère de la Basse Rusizi (Burundi). Ph.D. Thesis, Université Mohammed V de Rabat, Rabat, Morocco, 2022.
17. Domenico, P.A.; Schwartz, F.W. *Physical and Chemical Hydrogeology*; Wiley: New York, NY, USA, 1998; Volume 506.
18. Appelo, C.A.J.; Postma, D. *Geochemistry, Groundwater and Pollution*, 2nd ed.; Balkema: Rotterdam, The Netherlands, 2005.
19. Dassargues, A. *Hydrogeology: Groundwater Science and Engineering*; Taylor & Francis CRC Press: Boca Raton, FL, USA, 2018.
20. Walraevens, K.; Bakundukize, C.; Mtoni, Y.E.; Van Camp, M. Understanding the hydrogeochemical evolution of groundwater in Precambrian basement aquifers: A case study of Bugesera region in Burundi. *J. Geochem. Explor.* **2018**, *188*, 24–42. [CrossRef]
21. Aghazadeh, N.; Chitsazan, M.; Golestan, Y. Hydrochemistry and quality assessment of groundwater in the Ardabil area, Iran. *Appl. Water Sci.* **2017**, *7*, 3599–3616. [CrossRef]
22. Kumar, H.; Saini, V.; Kumar, D.; Chaudhary, R.S. Influence of trisodium phosphate (TSP) antiscalant on the corrosion of carbon steel in cooling water systems. *IJCT* **2009**, *16*, 401–410.
23. Fisher, R.S.; Mullican, W.F., III. Hydrochemical evolution of sodium-sulfate and sodium-chloride groundwater beneath the northern Chihuahuan Desert, Trans-Pecos, Texas, USA. *Hydrogeol. J.* **1997**, *5*, 4–16. [CrossRef]
24. Garrels, R.; Mackenzie, F. Origin of the Chemical Compositions of Some Springs and Lakes. *Am. Chem. Soc. Adv. Chem. Ser.* **1967**, *67*, 222–242. [CrossRef]

25. Gibbs, R.J. Mechanisms controlling world water chemistry. *Science* **1970**, *170*, 1088–1090. [CrossRef] [PubMed]
26. WHO. Guidelines for Drinking-Water Quality, 4th Edition, Incorporating the 1st Addendum. 2017. Available online: https://www.who.int/publications-detail-redirect/9789241549950 (accessed on 21 March 2022).
27. Debieche, T.H. Evolution de la qualité des eaux (salinité, azote et métaux lourds) sous l'effet de la pollution saline, agricole et industrielle: Application à la basse plaine de la Seybouse Nord-Est algérien. Ph.D. Thesis, Franche-comté University, Besançon, France, 2002.
28. Fetter, C.W. *Applied Hydrogeology*, 4th ed.; Pearson International Edition; Prentice Hall: Hoboken, NJ, USA, 2001.